JOURNAL OF SOLID STATE CHEMISTRY 63, 258–266 (1986)

S *K* and P *K* Absorption Spectra and Electronic Structures of Layered Thiophosphates MPS_3

YOUICHI OHNO

Department of Physics, Faculty of General Education, Utsunomiya University, Mine-machi 350, Utsunomiya 321, Japan

AND KIMIAKI HIRAMA

Nichiden Varian Company Ltd., Fuchu, Tokyo 183, Japan

Received September 3, 1985; in revised form November 15, 1985

The S *K* and P *K* absorption spectra of layered thiophosphates MPS_3 (M = Mg, Mn, Fe, Ni, Zn, Cd, Sn) were measured. The general features of the S *K* absorption spectra resemble one another, but the intensity ratio of the first peak to a higher energy structure and the energy position of a shoulder vary, depending on the metal species. All the P K absorption spectra exhibit a prominent peak in the neighborhood of the threshold. It is found that (1) the spectra mainly reveal the *p*-like partial density of states of the unoccupied energy levels of a $[P_2S_6]^{4-}$ cluster and (2) the first peak arises predominantly from the electronic transitions to the antibonding levels of the P–S bonds. The electronic structures and the optical spectra are discussed. © 1986 Academic Press, Inc.

Introduction

It is known that the layered thiophosphates denoted by the formula MPS_3 are synthesized over a wide range of metal elements in the periodic table. Up to date, it has been ascertained that the elements such as Mg, Ca, V, Mn, Fe, Co, Ni, Zn, Pd, Cd, Sn, Hg, and Pb form the compounds of this type (*1, 2*). Among them the elements except for Pd possess two electrons in the outermost shell, and no syntheses have been reported for the elements having one or three valence electrons in the outermost shell. Pd lies in the same column as Ni in the periodic table, but the 4*d* shell is completely filled by 10 electrons.

The magnetic studies (*3–5*) indicated that the metal atoms in first-row transition-metal thiophosphates exist as high-spin divalent ions. The infrared and Raman spectra (*6, 7*) showed that these compounds are composed of distorted $[P_2S_6]^{4-}$ clusters and that the covalent P—S bond strength is more predominant than that of the P—P bond. The crystal structure, which has been determined by Klingen *et al.* (*2, 8*) is related to the $CdCl_2$ structure (Fig. 1). The single crystal is constructed of a stack of sandwich layers. Each layer is weakly bonded by van der Waals forces. The intralayer structure is quite similar to that of TiS_2, one of group IV layered transition-metal disulfides. The only difference is that one P_2 pair occupies one of three Ti sites of the latter compound. Hence, we may expect two-dimensional electrical, magnetic, and optical properties. In fact, the magnetic

0022-4596/86 $3.00

Copyright © 1986 by Academic Press, Inc.
All rights of reproduction in any form reserved.

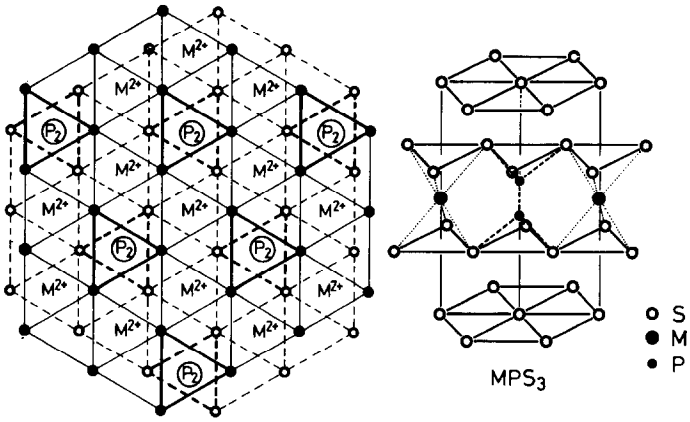

FIG. 1. Crystal structure of MPS_3.

structures of first-row transition-metal thiophosphates show a two-dimensional antiferromagnetic ordering (*5*).

The other important feature is that foreign atoms and molecules can be intercalated in the cationic forms into van der Waals gaps (*9–12*). Lithium-intercalated derivatives are especially important because it is possible to use them as cathods in secondary batteries (*13*). Many studies have been done in this aspect (*14–18*).

Although the electrical and optical studies (*4*) have indicated that they are wide-gap semiconductors or insulators, a full knowledge about the electronic structures has not been obtained. A simple and qualitative energy band scheme has been proposed in terms of the molecular orbital theory (*19, 20*), but no band calculations have yet been carried out. Because the reflectivity spectra of $MnPS_3$, $FePS_3$, and $NiPS_3$ exhibited similar structures, regardless of metal species, Khumalo and Hughes (*20*) predicted the band structures to be similar to one another and proposed an extremely ionic band model with localized metal 3*d* levels. Recently, Piacentini *et al.* (*19, 21*) and Kelly *et al.* (*22*) independently measured the photoemission spectrum of $NiPS_3$ to investigate the electronic structures of the valence band and the core levels. The former also carried out the measurements of the absorption spectra of $FePS_3$ and $NiPS_3$ by means of a partial yield technique to obtain information about the empty band structures. The results suggested that the valence band consists of the localized metal *d* levels, the S and P 3*s* levels, the S nonbonding *p* levels, and the bonding *p* levels derived from the P—S bonds, while the lowest conduction band is mainly made up of the P 3*s* antibonding orbitals.

In this paper, the S *K* and P *K* absorption spectra of a series of layered thiophosphates MPS_3 (*M* = Mg, Mn, Fe, Ni, Zn, Cd, Sn) are presented, and the electronic structures and the optical properties are discussed.

Experiments

(*1*) *Sample preparations.* All the samples were prepared by chemical vapor transport reactions of a stoichiometric amount of elements. The conditions of the crystal growth have been given by Klingen *et al.* (*2*). When Mg, Mn, Fe, Ni, Zn, and Cd were used as a metal element, large single crystals grew at the low-temperature region of an evacuated and then closed silica ampoule. No single crystal and no single-phase powder were obtained when using V and Co as a metal

element. Small plate-like crystals grew in the ampoules including Sn and Pd elements, but in this case most of the materials remained in the form of powder in the high-temperature region of the ampoule even after 3 weeks.

The synthesized crystals were investigated by an X-ray powder diffraction method. It was ascertained that the resulting compounds, except for the Pd derivative, are layered thiophosphates denoted by the chemical formula MPS_3. The lattice constants are in agreement with those of Klingen *et al.* (*2*), Taylor *et al.* (*3*), and Nitsche and Wild (*24*). The Pd derivative crystallized in the form of red–purple platelets with hexagonal symmetry. From the X-ray analysis, it has been confirmed that the derivative is not $PdPS_3$, but is $Pd_3(PS_4)_2$. The lattice constants are $a = 6.84$ Å and $c = 7.24$ Å, and the cleavage face is perpendicular to the c axis. We could not obtain the diffraction pattern for the single crystal of $SnPS_3$ because only a small number of crystals were grown. However, it was found from the analysis of the powder material that the resulting compound is of the second type (*2*) of monoclinic system.

$MgPS_3$ is so unstable that the fine powder rapidly changes color from transparent to white. Although this change is attributed to the hydrate formed by the reaction with the atmosphere, the X-ray diffraction pattern of the resulting complex still exhibits the strong and sharp ($00l$) lines which give the c lattice parameter enlarged only by less than 0.05 Å. Hence we consider that the above change is due to the intercalation of $MgPS_3$ with water molecules in the atmosphere.

(*2*) *X-Ray absorption measurements.* The measurements of the S K and P K absorption spectra of MPS_3 (M = Mg, Mn, Fe, Ni, Zn, Cd, Sn) and $Pd_3(PS_4)_2$ were carried out using a vacuum soft X-ray spectrometer of Johan type with a Rowland circle of the radius of 30 cm. All the X-ray absorption samples, except for $SnPS_3$ and $Pd_3(PS_4)_2$, were prepared in the form of a thin film by cleaving a single crystal in air by the use of adhesive tape. On the other hand, the samples of $SnPS_3$ and $Pd_3(PS_4)_2$ were prepared by rubbing fine powder onto a sheet of thin paper. These samples were quickly inserted into the specimen chamber which was then evacuated to 2×10^{-6} Torr to minimize the reaction with the atmosphere. The anode and filament materials of the X-ray tube were tungsten. The dispersing crystal was quartz with a $(10\bar{1}1)$ plane for the measurements of S K absorption spectra and with a $(10\bar{1}0)$ plane for the measurements of P K absorption spectra. The operating conditions of the X-ray tube were 4.3 kV and 30 mA for S K absorption measurements and 4.0 kV and 30 mA for P K absorption measurements. The transmitted and then dispersed X-rays were detected by a gas-flow proportional counter. The detected photon signals passing through a preamplifier and a pulse-height analyzer were integrated by a scaler during the preset time of 30–40 sec and then were printed out automatically on both a printer and an X-T recorder. The whole spectrum was obtained by means of a step scanning method. One unit step was chosen to correspond to the energy interval of 0.29 eV in both P K and S K spectra. The final spectrum was drawn on an X-Y plotter as normalized optical density versus energy by accumulating 3–5 data sets for each sample and processing them with a computer. Here the normalized optical density is given by

$$J(E) = \frac{\{\log(I_0(E)/I(E)) - \log(I_0(E_n)/I(E_n)\}}{\{\log(I_0(E_p)/I(E_p)) - \log(I_0(E_n)/I(E_n))\}},$$

where $I_0(E)$ and $I(E)$ are the intensities of the incident and the transmitted beams at energy E, respectively, and E_p and E_n are the energies at which maximum and no absorption occurs. The energy resolution, which includes the instrumental resolution

and the natural linewidth of the core level, is about 1.2 eV for both spectra.

Results and Discussion

Figures 2 and 3 show the S K absorption spectra of layered thiophosphates MPS_3 (M = Mg, Mn, Fe, Ni, Zn, Cd, Sn) and $Pd_3(PS_4)_2$. The corresponding P K absorption spectra are shown in Figs. 4 and 5.

The crystal of $Pd_3(PS_4)_2$ is transitional between layer type and three-dimensional, and the structure belongs to the trigonal space group D^3_{3d} (*25*). Each P atom is coordinated to four S atoms on the vertexes of a trigonal pyramid. Three of the P-S distances are 2.10 Å and the fourth is 2.00 Å. If the fourth S atom is substituted by a P atom, the remaining S and P atoms have the same coordination as those in MPS_3. Each Pd atom is surrounded by four S atoms on vertexes of a fairly regular square. This co-

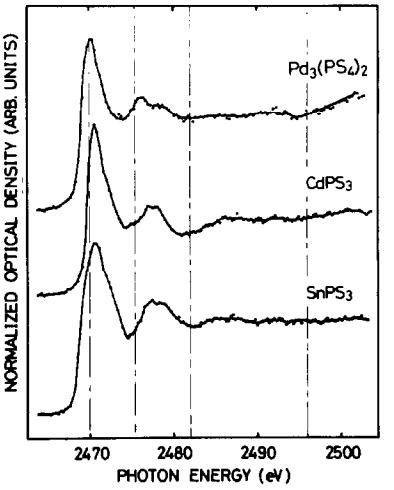

FIG. 3. S K absorption spectra of $CdPS_3$, $SnPS_3$, and $Pd_3(PS_4)_2$. Chain lines are drawn to aid in the comparison of the energy positions of the corresponding features. The energy at each chain line is the same as that of the corresponding line in Fig. 2.

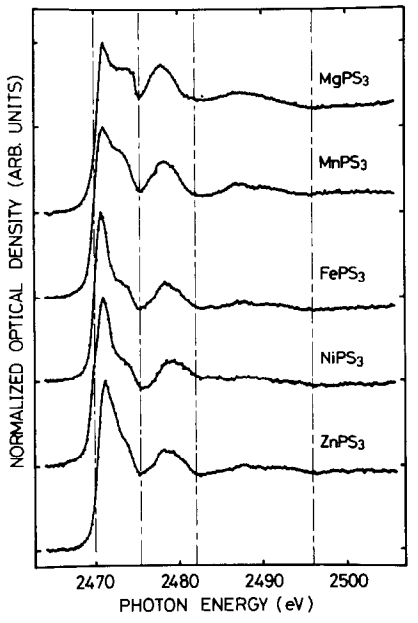

FIG. 2. S K absorption spectra of MPS_3 (M = Mg, Mn, Fe, Ni, Zn). Chain lines are drawn to aid in the comparison of the energy positions of the corresponding features.

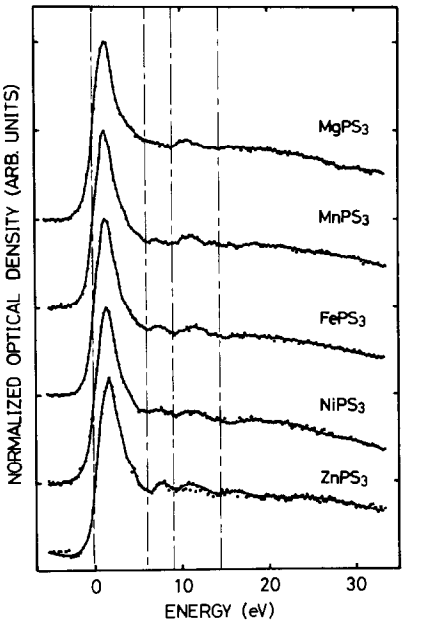

FIG. 4. P K absorption spectra of MPS_3 (M = Mg, Mn, Fe, Ni, Zn). Chain lines are drawn to aid in the comparison of the energy position of the corresponding features.

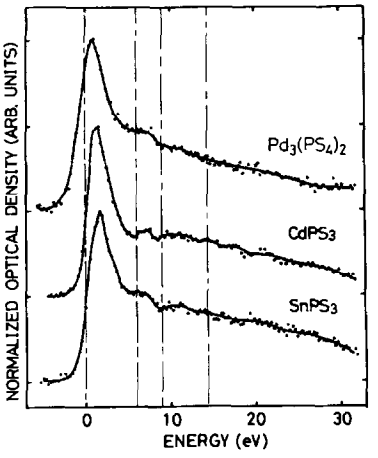

FIG. 5. P K absorption spectra of $CdPS_3$, $SnPS_3$, and $Pd_3(PS_4)_2$. Chain lines are drawn to aid in the comparison of the energy positions of the corresponding features. The energy at each chain line is the same as that of the corresponding line in Fig. 4.

ordination is very different from that of a metal atom in MPS_3. The latter metal atom is octahedrally coordinated to six S atoms.

As can be seen from Figs. 4 and 5, all the P K absorption spectra exhibit quite similar structures. The first peak near the threshold is prominent. The energy positions of the absorption edges agree within the errors except for $Pd_3(PS_4)_2$. The energies in the figures are referred to the position of the absorption edge of $MgPS_3$. The S K absorption spectra also resemble one another, but the intensity ratio of the first peak to a higher energy structure depends on the metal species and a shoulder structure around 2473 eV becomes dim with increasing the atomic number of the metal atom. The absolute photon energies were obtained by using the energy of the S K absorption edge of TiS_2 (*26*) as a reference. The energy position of the S K absorption edge is in good agreement among the first-row transition-metal thiophosphates, but it shifts to lower energies in the cases of $CdPS_3$, $SnPS_3$, and $Pd_3(PS_4)_2$ and to higher energy in the case of $MgPS_3$. However, these shifts do not depend on the electron occupancy of the metal d levels. Most of the results obtained support the earlier conclusions by Piacentini *et al.* (*23*) that the layered thiophosphates are composed of isolated metal ions and $[P_2S_6]^{4-}$ clusters, and that the near-edge structures of both S and P absorption spectra mainly represent the electronic structures of their clusters. However, the variations in intensity ratios of the first peak to a higher energy structure of the S K absorption spectra with the change of the metal species may imply that S atoms are under the larger influence of metal ions than P atoms are.

The S K and P K absorption spectra of $FePS_3$ will be compared with the S $L_{2,3}$ and P $L_{2,3}$ absorption spectra to investigate the character of the lowest conduction band (Fig. 6). The latter two absorption spectra have been obtained by Piacentini *et al.* (*23*) using a partial yield technique. When unoccupied s and p atomic wavefunctions are admixed within the conduction bands, the spectra are usually compared with one an-

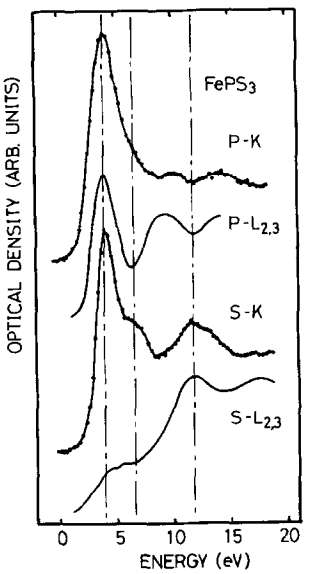

FIG. 6. P K, P $L_{2,3}$, S K, and S $L_{2,3}$ absorption spectra of $FePS_3$. The $L_{2,3}$ absorption spectra have been obtained by Piacentini *et al.* (*23*) by means of partial yield synchrotron-radiation photoemission spectroscopy.

other, aligning the absorption edges, because their positions correspond to the bottom of the conduction band. In the present case, however, the S K, P K, and P $L_{2,3}$ spectra are drawn by aligning the first peaks, assuming that the lowest conduction band consists of the molecular orbital levels of a $[P_2S_6]^{4-}$ cluster. The S $L_{2,3}$ spectrum is plotted on the figure in such a way that the structures around 3 and 11 eV above the threshold correspond to the peaks of the S K spectrum as well as possible. These procedures lead to the agreement of the absorption edges or the midpoints of the initial rise of absorption within 0.3 eV. Since the dipole selection rules hold satisfactorily in the X-ray absorption process, one can regard that the K absorption spectra reveal the local projected density of states with p symmetry near the absorbing atoms, while the $L_{2,3}$ absorption spectra reveal the local projected density of states with s and d symmetries near the absorbing atoms. The intensity ratios of the first peak to a higher energy structure of these spectra suggest that the lowest conduction band consists of dense S p and P s and p states. The result is easily predicted from a simple molecular orbital model of a $[P_2S_6]^{4-}$ cluster. Mathey and co-workers (*6, 7*) have indicated from Raman and infrared spectra that the strength of the covalent P—S bonds in a $[P_2S_6]^{4-}$ cluster are more predominant than that of the P—P bond. The valence electrons of a S and a P atom are $3s$ and $3p$ electrons. The P s character, which is deduced from the P $L_{2,3}$ spectrum, is included in the antibonding energy levels together with a P p character through the sp^2 hybridized orbitals which are most appropriate to form the covalent P—S bonds with surrounding three S atoms. A remaining $3p$ orbital in a P atom is used to form the P—P bond. This bond plays a role of the connector of two PS_3 entities in a $[P_2S_6]^{4-}$ cluster. On the other hand, a S atom expends a $3p$ orbital on the bonding with a P atom, but the remaining $3s$ and $3p$ orbitals take no part in the bonding and exist as a nonbonding orbital. This bonding scheme implies that the unoccupied energy states of this cluster consist of the antibonding orbitals of the P—S and P—P bonds. The electron occupancy of the P—S antibonding levels per double formula is twelve, and is much larger than two of the P—P antibonding levels. Thus we may conclude that the first absorption peak arises mainly from the transitions to the P—S antibonding states which contain P s, P p, and S p characters. This conclusion is supported by the present experimental results.

With respect to the peak and dip positions of the higher energy structures, there is an agreement between the spectra obtained from the same kind of absorbing atoms, for example, between the P K and P $L_{2,3}$ spectra, but a disagreement is found between the S and P spectra. This fact may suggest that these structures are derived from the transitions to the excited states of each atom, but the details are unknown at present. In relation to this problem, we may need to take account of the mixture bands with unoccupied metal s and p orbitals and the photoelectron multiple-scattering effect. In the continuous levels around 15 eV above the edge, the photoelectron multiple-scattering effect becomes relatively important because the density of states are smoothly varied.

Next, we will discuss the electronic structures and the optical spectra. Figure 7 shows the S K and P K absorption spectra of $NiPS_3$ together with the valence band photoemission spectrum. This photoemission spectrum has been measured by Kelly *et al.* (*22*) at the photon energy of 55 eV. According to Kelly *et al.*, the peaks A, B, and C are related to the Ni $3d$ levels, while the peak D is assigned to the $p_{x,y}$ levels, although the photon polarization effect has shown that this peak has a p_z character perpendicular to the layers rather than a $p_{x,y}$

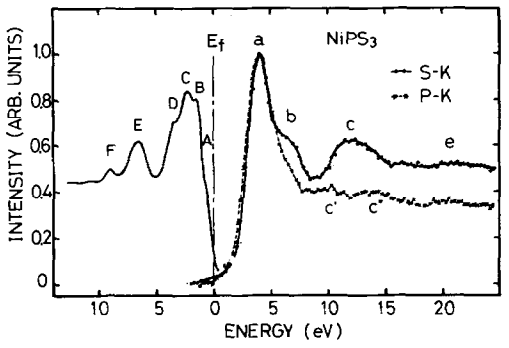

FIG. 7. S K and P K absorption spectra and the valence band photoemission spectrum of $NiPS_3$. The photoemission spectrum (solid line) has been obtained by Kelly *et al.* (*22*). The spectra are drawn in such a way that the electron transitions D → a and E → a, respectively, give rise to the prominent peaks around 7.5 and 10 eV of the reflectivity spectrum measured by Khumalo *et al.* (*20*).

character parallel to the layers. Since the peak E exhibited the resonant behavior, it was regarded as a satellite of the Ni 3*d* levels. On the other hand, Piacentini *et al.* (*21*) have asserted that the peaks D and E reveal the S $p_{x,y}$ nonbonding levels and the bonding levels derived from the P—S bonds, respectively, by measuring the photoemission spectra of the familiar compounds and comparing with them. The peak F was ascribed to the contaminated oxygen peak, but its nature remained uncertain because it appeared even after cleavage under ultrahigh vacuum conditions. These assignments were done in terms of the simple molecular orbital model proposed by Piacentini *et al.* (*19*). However, there are some questionable points in this model. For example, the antibonding $p_{x,y}$ level which is derived from a covalent P—S bond, is situated below the Fermi level. If it is right, the P—S bond is unstable because valence electrons occupy both the bonding and the antibonding states. The Raman and infrared studies (*6*) have confirmed the strong P—S bond. The force constant has been estimated to be 2.30 mdyn/Å. Thus we believe that the antibonding level is situated above the Fermi level and that the electronic transitions to the antibonding level give rise to the first peak of the S K and P K absorption spectra as described above.

Khumalo and Hughes (*20*) measured the reflectivity spectra of $MnPS_3$, $FePS_3$, and $NiPS_3$. They noted two prominent peaks; one is a sharp peak around 7.5 eV and the other is a relatively broad peak around 10 eV. Since the peaks appeared, irrelevant to the metal species, Khumalo and Hughes (*20*) related them with the electronic transitions from the occupied to the unoccupied energy states of $[P_2S_6]^{4-}$ clusters. As described above, the unoccupied energy states of $[P_2S_6]^{4-}$ clusters show a prominent peak near the bottom of the conduction band, while the occupied states exclusive of metal 3*d* states exhibit two large peaks at 3.0 and 6.0 eV below the Fermi level. These peaks are, respectively, related to the P—S antibonding levels, the nonbonding S 3*p* levels, and the P—S bonding levels in order. Then we may assume that the former peak of the reflectivity spectra arises from the electronic transitions from the nonbonding S 3*p* levels to the P—S antibonding levels, while the latter peak arises from the electronic transitions from the bonding to the antibonding levels of the P—S bonds. Figure 7 is drawn for $NiPS_3$, paying attention to the points that the transitions D → a and E → a give rise to the prominent peaks around 7.5 and 10 eV in the reflectivity spectrum. We find that the Fermi level or the top of the valence band is situated below the S K and P K absorption edges. This means that $NiPS_3$ is a semiconductor, in agreement with the result of the optical absorption study (*4*). However, this procedure gives a somewhat larger energy gap than the fundamental absorption edge. According to Brec *et al.* (*4*) the fundamental absorption edge of $NiPS_3$ is 1.6 eV, while the energy separation between the top of the valence band and the bottom of the conduction band in Fig. 7 is about 2.6 eV. It is

known that Ni 3*d* levels play an important role for the optical transitions at low energies, but the unoccupied Ni 3*d* levels are not shown in the figure because the S *K* and P *K* absorption spectra give no information about the metal 3*d* levels. If the unoccupied Ni 3*d* levels are considered, it might be possible to correct the above disagreement. Although we tried to obtain information about the ground states of the unoccupied metal 3*d* levels of $MnPS_3$, $FePS_3$, and $NiPS_3$ by measuing the metal $L_{2,3}$ absorption spectra, this attempt resulted in a failure due to the strong interaction between a core 2*p* hole and the 3*d* electrons (*27*). In this attempt we observed the multiplet splitting of the final states of a divalent metal ion which implies the presence of the strongly localized metal 3*d* electrons. On the other hand, in $ZnPS_3$ where the 3*d* levels are situated sufficiently below the Fermi level, there is a good agreement between the fundamental absorption edge and the energy separation between the top of the valence band and the bottom of the conduction band which has been estimated in the same procedure as done for $NiPS_3$. In this case, the valence band photoemission spectrum and the reflectivity spectrum have been quoted from Ref. (*21*).

Putting the above discussions together, we can obtain the energy level scheme as shown in Fig. 8. This scheme is constructed of the energy levels of $[P_2S_6]^{4-}$ clusters and the localized 3*d* levels of divalent metal ions. Taking no account of the metal 3*d* levels, the top of the valence band and the bottom of the conduction band consist of the bonding and the antibonding levels derived from the P—P bonds, respectively. The direct evidence of the existence of the P—P bond has been given by the infrared study (*6*), which suggests that the bond strength is considerably smaller than those of P_2 and P_4 molecules. These densities of states are much lower, so that they could not be identified from the photoemission and the X-ray absorption spectra.

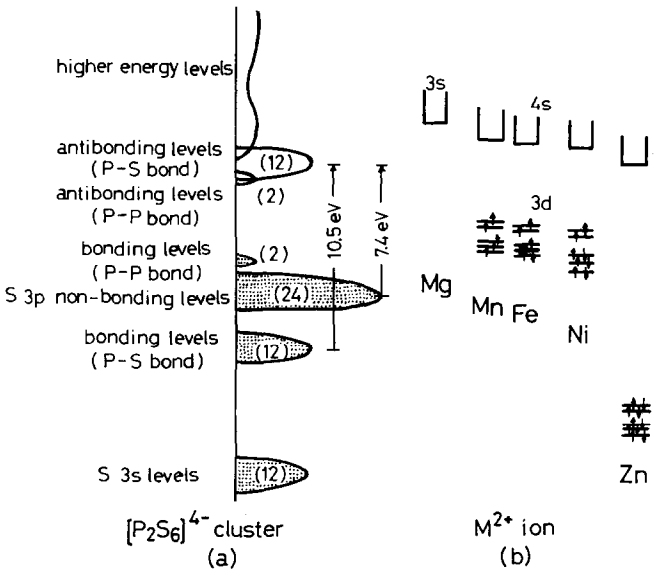

FIG. 8. Energy level scheme of MPS_3. It is constructed of the energy levels of $[P_2S_6]^{4-}$ clusters (a), and localized divalent metal ions (b). The figures in parentheses denote the electron occupancy per double formula and dots show occupied states. The *d* electrons in first-row transition-metal ions are localized in a high-spin state, while the 4*s* orbitals are delocalized and interact with sulfur *s* and *p* orbitals.

Until now, we have neglected the interaction between a localized divalent metal ion and a $[P_2S_6]^{4-}$ cluster, but weak mixing may occur between the delocalized metal s and p orbitals and the S 3*p* nonbonding orbitals because the latter orbitals are directed to the metal atoms. Even if so, the present authors believe that the layered thiophosphates are stabilized by the two-dimensional arrangement of isolated divalent metal cations and strongly bonded $[P_2S_6]^{4-}$ anions. The *M*—S and *M*—*M* interactions may play a role for the lower energy shifts of the S *K* and P *K* absorption spectra of $Pd_3(PS_4)_2$ and $SnPS_3$. As the interactions increase, the resulting complexes would exhibit three-dimensional properties rather than two-dimensional properties.

Conclusions

The S *K* and P *K* absorption spectra of a series of layered thiophosphates MPS_3 (*M* = Mg, Mn, Fe, Ni, Zn, Cd, Sn) were obtained. The whole energy level scheme was drawn by taking account of the valence band photoemission and the X-ray absorption spectra. This scheme is constructed of the energy levels of $[P_2S_6]^{4-}$ clusters and the localized *d* levels of divalent metal ions. It will be useful not only for the assignments of the structures of the reflectivity spectra and the optical adsorption spectra, but also for the execution of the band calculations.

Acknowledgment

This work partially supported by a Grant in Aid for Scientific Research from the Ministry of Education of Japan.

References

1. F. Hulliger, *in* "Physics and Chemistry of Materials with Layered Structures" (F. Lèvy, Ed.), Vol. 5, p. 217, Reidel, Dordrecht/Boston/London (1976).
2. W. Klingen, R. Ott, and H. Hahn, *Z. Anorg. Allg. Chem.* **396,** 271 (1973).
3. B. E. Taylor, J. Steger, and A. Wold, *J. Solid State Chem.* **7,** 461 (1973).
4. R. Brec, D. M. Schleich, G. Ouvrard, A. Louisy, and J. Rouxel, *Inorg. Chem.* **18,** 1814 (1979).
5. G. LeFlem, R. Brec, G. Ouvrard, A. Louisy, and P. Segransan, *J. Phys. Chem. Solids* **43,** 455 (1982).
6. Y. Mathey, R. Clement, C. Sourisseau, and G. Lucazeau, *Inorg. Chem.* **19,** 2773 (1980).
7. C. Sourisseau, J. P. Forgerit, and Y. Mathey, *J. Solid State Chem.* **49,** 134 (1983).
8. W. Klingen, G. Eulenberger, and H. Hahn, *Z. Anorg. Allg. Chem.* **401,** 97 (1973).
9. R. Clement and M. L. H. Green, *J. Chem. Soc. Dalton Trans.* **10,** 1566 (1979).
10. J. P. Audiere, R. Clement, Y. Mathey, and C. Mazieres, *Physica B & C* **99,** 133 (1980).
11. C. Sourisseau, Y. Mathey, and C. Poinsigon, *Chem. Phys.* **71,** 257 (1982).
12. C. Sourisseau, J. P. Forgerit, and Y. Mathey, *J. Phys. Chem. Solids* **44,** 119 (1983).
13. A. H. Thompson and M. S. Whittingham, *Mater. Res. Bull.* **12,** 741 (1977).
14. C. Berthier, Y. Chabre, and M. Minier, *Solid State Commun.* **28,** 327 (1978).
15. R. Brec, G. Ouvrard, A. Louisy, J. Rouxel, and A. Le Mehaute, *Solid State Ionics* **6,** 185 (1982).
16. P. J. S. Foot and B. A. Nevett, *Solid State Ionics* **8,** 169 (1983).
17. M. Barj and G. Lucazeau, *Solid State Ionics* **9, 10,** 475 (1983).
18. M. Barj, C. Sourisseau, G. Ouvrard, and R. Brec, *Solid State Ionics* **11,** 179 (1983).
19. M. Piacentini, F. S. Khumalo, C. G. Olson, J. W. Anderegg, and D. W. Lynch, *Chem. Phys.* **65,** 289 (1982).
20. F. S. Khumalo and H. P. Hughes, *Phys. Rev. B.* **23,** 5375 (1981).
21. M. Piacentini, F. S. Khumalo, G. Leveque, C. G. Olson, and D. W. Lynch, *Chem. Phys.* **72,** 61 (1982).
22. M. K. Kelly, R. R. Daniels, G. Margaritondo, and F. Lèvy, *Solid State Commun.* **50,** 233 (1984).
23. M. Piacentini, V. Grasso, S. Santangelo, M. Fanfoni, S. Modesti, and A. Savoia, *Solid State Commun.* **51,** 467 (1984).
24. R. Nitsche and P. Wild, *Mater. Res. Bull.* **5,** 419 (1970).
25. T. A. Bither, P. C. Donohue, and H. S. Young, *J. Solid State Chem.* **3,** 300 (1971).
26. Y. Ohno, K. Hirama, S. Nakai, C. Sugiura, and S. Okada, *Phys. Rev. B* **27,** 3811 (1983).
27. Y. Ohno and S. Nakai, *J. Phys. Soc. Japan* **54,** 3591 (1985).